PAPER • OPEN ACCESS

Molecular dynamics simulations of the monomer density profiles of knotted ring polymer chains confined in a slit of two parallel walls with one attractive and another repulsive surface.

To cite this article: P Kuterba *et al* 2023 *J. Phys.: Conf. Ser.* **2436** 012031

View the article online for updates and enhancements.

Molecular dynamics simulations of the monomer density profiles of knotted ring polymer chains confined in a slit of two parallel walls with one attractive and another repulsive surface.

P Kuterba[1], H Christiansen[2], Z Danel[3] ∗ and W Janke[2]

[1] Institute of Physics, Jagiellonian University, st. prof. S. Łojasiewicza 11, 30-348 Kraków, Poland

[2] Institut für Theoretische Physik, Universität Leipzig, IPF 231101, 04081 Leipzig, Germany

[3] Faculty of Materials Engineering and Physics, Cracow University of Technology, st. Podchorążych 1, 30-084 Kraków, Poland

E-mail: piotr.kuterba@uj.edu.pl

Abstract. We have used Molecular Dynamics simulations to obtain the monomer density profiles for real linear and ring polymer chains of 360 monomers length with different topological structures such as simple knots: 3_1, 6_1, 9_1, 10_{124}, complex knots $3_1 3_1 5_1$ and twisted knots with $n = 10$ and $n = 20$ in a slit geometry of two parallel walls with one attractive and another repulsive surface. We have used Large-scale Atomic/Molecular Massively Parallel Simulator (LAMMPS) software to perform simulations with the Verlet integration algorithm. The interactions between monomers were simulated as Lennard-Jones 12-6 potential, for bonds we have used Finitely Extensible Nonlinear Elastic (FENE) potential and the interaction with the walls was taken into account via Lennard-Jones 9-3 potential. We observed that topologically complex polymers have lower monomer density profiles near the attractive wall, but at some distance in the direction to the repulsive wall this tendency changes to the opposite. We showed that most complex twisted knots have two maxima in narrow slits. In the wide slits we do not observe such relation for twisted knots at higher temperatures. These results are important for better understanding the nature of the depletion forces which arise in a slit geometry of two parallel walls with one attractive and one repulsive wall.

1. Introduction

One distinguishing property of polymers is their length, which makes them different from other molecules and from which the most of the important polymer specific properties arise. Due to thermal fluctuations, they, for example, can penetrate large volumes. These volumes can be either unconstrained or constrained. The constrained volumes naturally have different geometries of the surrounding surfaces, for example, consisting of planar walls (either only a single wall or, as in our case, two walls), spherical and many other combinations. They are usually chosen in such a way that it is an approximation of a natural structure.

However, the solutions can have different properties depending on the topological structure of the dissolved polymers. The polymers can, for example, be linear, a simple ring, or an entangled

∗Previously Z. Usatenko

ring. Knotted ring polymers are a special type of polymers that can have a few interesting properties that make them interesting to study.

Biopolymers such as DNA very often present a ring topology, as it was shown in a series of the atomic force spectroscopy (AFM) experiments [1, 2]. Such, for example, Escherichia coli (E. coli) bacteria which is resistant to a wide spectrum of antibioticshas has a ring topology [3]. The biopolymers of the DNA of some viruses such as bacteriophages λ that infect and destroy E. coli bacteria oscillate between a linear and ring topology [4, 5]. Mature viruses have the linear form of DNA, but inside of the host cell DNA of bacteriophages adopts a ring topology [6]. Such an investigation is important in the context of understanding the processes that lead to the destruction of E. coli bacteria with the help of bacteriophages λ and in the context of creating phage-therapy, which is an alternative way to antibiotic treatment, especially in the case of bacteria that demonstrate high resistance to antibiotics. Besides, confinement and chain topology play a significant role in the shaping of individual chromosomes and in the process of their segregation, as it was shown in [7].

In the bacterial biology chain topology and confinement can play a crucial role in shaping morphology of the chromosomes and their segregation [7]. It has been shown that under strong confinement conditions, topologically distinct domains of a polymer complex can repel each other maximizing conformational entropy. By entangling ring polymers in different ways, one introduces a topological change, effectively tuning the complexity of the polymer. Linear long polymers like DNA can entangle themselves, however, they can also disentangle. This is different for the ring polymer, which is entangled before the ends connect. Thus, it is impossible to disentangle it without breaking bonds in the chain. Such polymers were investigated in [5], where it was shown that in a narrow slit of two repulsive walls the more complex knots exert higher forces on the walls than comparable linear polymers. These fundamental topological differences between linear and ring polymer chains make it interesting from a theoretical, technological, or biological perspective.

The numerical results based on the MC simulations [8] suggest that the knotted ring polymers will exert higher entropic forces on the walls of the confining slit than unknotted or linear polymers. The molecular dynamics simulations performed in [5] allowed to obtain the entropic force exerted on the walls arising from the confinement to a slit of a knotted ring and the monomer density profiles in the case of two repulsive walls.

Recently, the effect of a nanoslit confinement on the topological properties of the circular model DNA, which was modeled as a semiflexible polymer chain were analysed in [9] by advanced MC simulation techniques. It was shown [9] that the knotting probability has strong slit width dependence. The investigation of the influence of topological constraints on the free energy and metric properties of an ideal ring polymer without excluded volume effects or attractive interactions confined in a narrow slit were performed in [10] using off-lattice MC simulations. The occurrence and behavior of polymer knots were studied extensively by MC simulations in [11, 12, 13, 14]. Thus in [11] was shown that the effective stiffening of DNA by the nematic arrangement promotes the formation of torus knots in phage capsids. It should be also noted that the conservation of the knot topology in simulations of ring polymers depends on the knotting probability of the knot, as was shown in [14] by the use of the self-avoiding polygons (SAPs) method.

In [15] the monomer density profiles of ring polymers with different topological structures between attractive and repulsive walls have been investigated analytically. It was shown that near an attractive wall, the monomer density profiles of complex ring polymers have lower absolute values than those of linear polymers. In this paper, we will focus on the calculation of the monomer density profiles of knotted ring polymers in confined geometries via Molecular Dynamics simulations. The polymers are placed in a slit of two parallel walls with the mixed boundary conditions mentioned above. Our investigations include calculations of the monomer

density profiles for different temperatures and different topological structures of ring polymers.

2. Model and Methods

In this study, we performed Molecular Dynamics simulation using LAMMPS (Large-scale Atomic Molecular Massively Parallel Simulator) [16] for ring polymers consisting of 360 monomers. Neighbouring-bead interactions were modeled with the FENE potential [20]:

$$U_{\text{FENE}}(r) = -\frac{KR_0^2}{2} \ln\left[1 - \left(\frac{r}{R_0}\right)^2\right], \tag{1}$$

for $r < R_0$, where $R_0 = 1.0$ and $K = 40.0$. In the region of $r > R_0$ the potential $U_{\text{FENE}}(r) = 0$. Repulsion between monomer pairs was modeled with a 12-6 Lennard-Jones (LJ) potential:

$$U_{\text{LJ}}(r) = 4\epsilon\left[\left(\frac{\sigma}{r}\right)^{12} - \left(\frac{\sigma}{r}\right)^6\right], \tag{2}$$

for $r \leq r_{\min}$, where $r_{\min}$ was obtained from the condition $dU_{\text{LJ}}(r)/dr = 0$ and equal $r_{\min} = 2^{\frac{1}{6}}\sigma$ with $\sigma = 0.7/2^{\frac{1}{6}} = 0.6236$ and $\epsilon = 1$. The potential was shifted $U_{\text{LJ,sh}}(r) = U_{\text{LJ}}(r) - U_{\text{LJ}}(r_{\min})$ in order to get $U_{\text{LJ,sh}}(r_{\min}) = 0$ and it was also truncated $U_{\text{LJ}}(r) = 0$ for $r > r_{\min}$. The interaction between monomer and a wall was taken into account via the LJ 9-3 potential [19]:

$$U_{\text{LJ}}^{\text{wall}}(z) = \epsilon_w\left[\frac{2}{15}\left(\frac{\sigma}{z}\right)^9 - \left(\frac{\sigma}{z}\right)^3\right], \tag{3}$$

where $z \leq z_c$, with $z_c = z_{\min}$, which was obtained from the condition $dU_{\text{LJ}}^{\text{wall}}(z)/dz = 0$ and equal $z_{\min} = \left(\frac{2}{5}\right)^{\frac{1}{6}}\sigma = 0.5353$ for the repulsive wall. At the attractive wall the potential was truncated at $z_c = 4.5\sigma$. Potentials on both walls have $\epsilon_w = 1.0$ and were additionally shifted and truncated according to $U_{\text{LJ,sh}}^{\text{wall}}(z) = U_{\text{LJ}}^{\text{wall}}(z) - U_{\text{LJ}}^{\text{wall}}(z_c)$, so that $U_{\text{LJ,sh}}^{\text{wall}}(z) = 0$ for $z \geq z_c$.

We have used the Verlet integration algorithm with the Langevin thermostat (with constant temperature) and the time step $\Delta t = 0.001$. The simulation equilibration time was 10^7 steps, and the simulation data was collected for over 2×10^7 steps. The monomer densities were averaged over 10 separate simulations. We have performed simulations for linear, ring polymers and the following knotted ring polymers in Alexander-Briggs notation c_p, where c is the number of crossings and p is the ordinal number: $3_1, 6_1, 9_1, 10_{124}, 3_1 3_1 5_1$ and twisted knots with $n = 10$ and $n = 20$ numbers of twists. Considered are two widths of the slits: a narrow slit with width $4.81\sigma = 3.0$ and a wide slit with width $19.24\sigma = 12$. We have also fitted the kernel functions and scaled the widths of both slits to one and plotted them as probability distribution functions.

3. Results

The monomer density profiles ρ for the polymers in a slit geometry of one repulsive and another attractive wall are presented in Fig. 1. On the horizontal axis z we can see the width of the slit scaled to one, where the attractive wall is placed at 0 and the repulsive wall at 1. In Fig. 1 we can see that in narrow slits the densities reach lower maximal values than in wide slits. The difference between maximal values of narrow and wide slits decreases with increasing the temperature.

At lowest temperature $T = 1.00$ the maximal absolute values of the monomer density profiles for the wide slit are around four times larger than for the narrow slit for all types of polymer structures. The linear and ring polymers with knots: 6_1, 9_1, 10_{124}, $3_1 3_1 5_1$ for narrow slits for all temperatures and wide slits at temperatures $T = 1.00$ and $T = 1.40$ have one maximum

near the attractive wall, from which it starts to monotonically decrease in the direction to the repulsive wall. In wide slits for temperatures $T = 2.00$, $T = 2.28$ and $T = 3.00$ the maximum values of the monomer densities move from the attractive wall closer to the middle of the slit. On the other hand, the twisted knots $n = 10$ and $n = 20$ have two local maxima, first a higher one closer to the attractive wall and second a lower one at some distance what is connected with the specific topological structure of the above mentioned polymers.

The monomer densities generally decrease with complexity near the attractive wall for all temperatures in narrow slits and $T = 1.00$, $T = 1.40$ for wide slits. At some point monomer densities cross and the behaviour changes to the opposite, where it increases with increasing complexity of the polymer. Such crossing for the narrow slit is around $z = 0.4$ at $T = 1.00$ and with increasing temperature increaes up to $z = 0.5$ at $T = 3.00$. In wide slits the crossing is closer to the attractive wall and is approximately near $z = 0.1$ at $T = 1.00$ and changes up to $z = 0.3$ at $T = 3.00$. It should be noted that the distance between the local maxima in the narrow slit for the twisted knots $n = 10$ and $n = 20$ is generally the same and is around 0.3 of the width of the slit, which is approximately 1.44σ, where σ is the monomer size. After considering the local maxima in the wide slit at $T = 1.00$ one can notice that the second is lower than the first and with increasing temperature it moves toward repulsive wall and the density plot in general flattens and extends over the slit. Interestingly, there is no such phenomenon for the narrow slit, where both maxima tend to similar values with increasing temperature. Another interesting observation can be made that the most complex twisted knots have at least
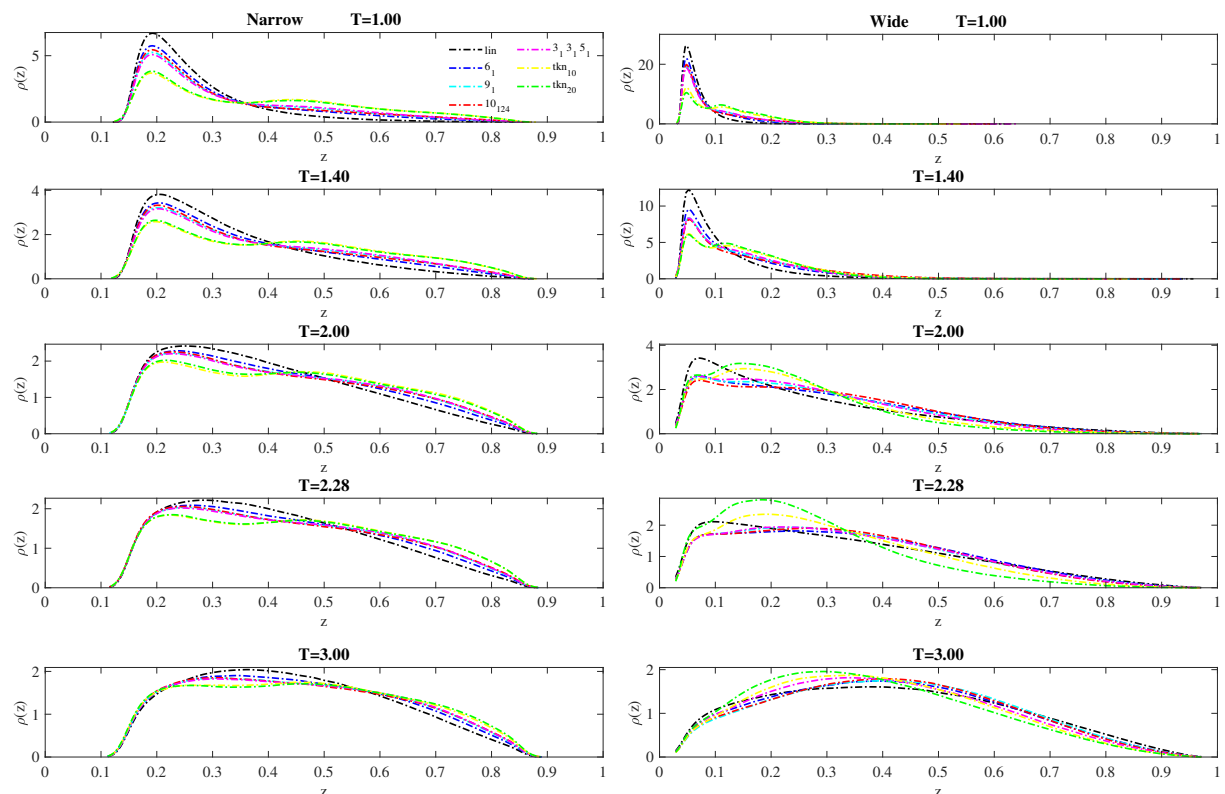

Figure 1. Monomer density profiles ρ for multiple entanglements in: (a) narrow 4.81σ and (b) wide slit 19.24σ for different reduced temperatures: $T = 1.00$, $T = 1.40$, $T = 2.00$, $T = 2.28$, $T = 3.00$. The horizontal axis is scaled to one and the attractive wall is set at 0 and the repulsive at 1.

two local maxima in the distribution for $T = 1.00$ and $T = 1.40$ for the narrow slit with large difference in their values. However, this difference for temperature $T = 2.00$ and above this difference decreases significantly reaching similar values at $T = 3.00$. In a wide slit the second maximum, as previously mentioned, at $T = 1.00$ is significantly lower than the first, but with increasing temperature it increases in relation to the first maximum. At some temperature, between $T = 1.40$ and $T = 2.00$ it becomes larger than the first maximum, extends its width and moves towards the repulsive wall. It is interesting that for temperatures $T \geq 2.00$ the first maximum, which was visible for lower temperatures is no more visible. It suggests that the first maximum, the closest to the attractive wall, is due to adsoption of the polymer on the wall and the number of the adsorbed monomers on the wall decreases at the cost of monomers fluctuating in the inner space of the slit. This observation could be extended over all polymers in the simulations. However the character of this change is different depending on the topology of the chain. One can notice that for the higher temperatures $T = 2.00$, $T = 2.28$ and $T = 3.00$ in wide slits, the density of complex polymers is lower than that of linear polymer chains in the vicinity of the repulsive wall. It is opposite to other temperatures for wide slit and all temperatures in narrow slit, and it is similar to previously described case of either increasing or decreasing monomer densities with complexity for the same temperatures, thus, both effects can have common source. It may be connected with the steric effects of some of the monomers closer to the attractive wall, where in complex polymers, the monomers can be blocked in that area by limited chain extension due to entanglements, and the linear polymer chains can extend themselves to larger distances.

4. Conclusions

In our study, we have investigated the monomer density profiles ρ of ring polymers with different topological structures across the slits in the space between two parallel walls with mixed boundary conditions for different temperatures. Thermal fluctuations in the system serve as the main driving force for the polymer to move in the slit. It is important because we can estimate whether the polymer actually interacts with certain system components or whether it can serve as a mediator of interaction between components like the walls. We can see that the polymers have higher densities near the attractive wall compared to the repulsive one, where it decreases. It should result in repulsive depletion force, which is important from a technological point of view as it can serve as a mediator in reducing the static friction in micro- and nano-electromechanical devices. These results are in agreement with the analytical predictions obtained in [15]. It should be mentioned that twisted knots have interestingly two local maxima, which is not the case for other polymers. With 360 monomers the length of the polymer is short compared to the number of crossings it has, which makes the polymer more tense than other less complicated ones. In such setup the second maximum could be explained simply by arising from intra chain steric effects, which orders the monomers and makes them more or less frequent at some volumes. There is an interesting difference in behaviour of the most complex twisted $n = 20$ polymer between narrow and wide slit. The second maximum for the wide slits can increase much faster and become larger than the first maximum with increasing temperature. However there is a qualitative difference in behaviour for narrow slits. In slits with small wall separation both maxima have some limiting value which both tend to reach, see twisted knot $n = 20$ in Fig. 1 for $T = 3.00$. Such behaviour could be related to the steric effects and the limited space that the complex polymer can occupy. This could lead to the situation where the polymer could be squeezed so much that the pair potential repulsion orders the monomers such that the slit width is fully occupied and thus present double domain [6] or a pseudocrystalline structure. Twisted knots have interesting topology that could be simply describedas an unknot ring twisted n times with far ends linked together [21] resembling two separate chains linked together. The two maxima in the monomer density profiles could be

explained by the topological structure of the polymers. It would be interesting in the future to increase the polymer length of the twisted knots with $n = 20$ and test if the second maximum vanishes for longer chains. Similarly it can be done for the less complicated polymers to check if such additional maxima would arise if the chain length would decrease enough. This could help to better understand the impact of the intra chain tension due to topological and steric effects together. Additionally, it has been shown recently in [22] that the coupling strength of the contour motion of the interlocked regions of the linked chains is universal to their size. So it would be also interesting to check if the coupling strentgh of the parts of the knotted polymers, especially twisted knots due to their specific topology, also have universal properties.

References

[1] Marek, J.; Demjénová, E.; Tomori, Z.; Janáček, J.; Zolotová, I.; Valle, F.; Favre, M. Interactive measurement and characterization of DNA molecules by analysis of AFM images. Cytom. Part A 2005, **63A**, 87.

[2] Witz, G.; Rechendorff, K.; Adamcik, J.; Dietler, G. Conformation of ring polymers in 2D constrained environments. Phys. Rev. Lett. 2011, **106**, 248301.

[3] Berg, J.; Tymoczko, J.; Stryer, L. Biochemistry, 5th ed.; Freeman W. H. and Co.: New York, NY, USA, 2002.

[4] Arsuaga, J.; Vazquez, M.; Trigueros, S.; Sumners, D.W.; Roca, J. Knotting probability of DNA molecules confined in restricted volumes: DNA knotting in phage capsids. Proc. Natl. Acad. Sci. USA 2002, 99, 5373–5377.

[5] Matthews, R.; Louis, A.A.; Yeomans, J.M. Confinement of knotted polymers in a slit. Mol. Phys. 2011, **109**, 1289.

[6] Miller, R.V. Bacterial gene swapping in nature. Sci. Am. 1998, **278**, 66.

[7] Jun, S.; Mulder, B. Entropy-driven spatial organization of highly confined polymers: Lessons for the bacterial chromosome. Proc. Natl. Acad. Sci. USA 2006, **103**, 12388.

[8] van Rensburg, E.J.J. Squeezing knots. J. Stat. Mech. 2007, 2007, P03001.

[9] Micheletti, C.; Orlandini, E. Numerical study of linear and circular model DNA chains confined in a slit: Metric and topological properties. Macromolecules 2012, **45**, 2113.

[10] Li, B.; Sun, Z.Y.; An, L.J.; Wang, Z.G. Influence of topology on the free energy and metric properties of an ideal ring polymer confined in a slit. Macromolecules 2015, **48**, 8675–8680.

[11] Reith, D.; Cifra, P.; Stasiak, A.; Virnau, P. Effective stiffening of DNA due to nematic ordering causes DNA molecules packed in phage capsids to preferentially form torus knots. Nucleic Acids Res. 2012, **40**, 5129.

[12] Trefz, B.; Siebert, J.; Virnau, P. How molecular knots can pass through each other. Proc. Natl. Acad. Sci. USA 2014, **111**, 7948–7951.

[13] Marenz, M.; Janke, W. Knots as a topological order parameter for semiflexible polymers. Phys. Rev. Lett. 2016, **116**, 128301.

[14] Erica, U.; Deguchi, T. Knotting probability of self-avoiding polygons under a topological constraint. J. Chem. Phys. 2017 **147**, 094901.

[15] Halun, J.; Karbowniczek, P.; Kuterba, P.; Danel, Z. Investigation of ring and star polymers in confined geometries: Theory and simulations. Entropy 2021, **23**, 242.

[16] Thompson, A. P.; Aktulga, H. M.; Berger, R.; Bolintineanu, D. S.; Brown, W. M.; Crozier, P. S.; in 't Veld, P. J.; Kohlmeyer, A.; Moore, S. G.; Nguyen, T. D.; Shan, R.; Stevens, M. J.; Tranchida, J.; Trott, C.; Plimpton, S. J., LAMMPS - a flexible simulation tool for particle-based materials modeling at the atomic, meso, and continuum scales, Comp Phys Comm, **271** 2022 10817.

[17] Nevers, Y.; Glover, N.; Dessimoz, C.; and Lecompte, O. Protein length distribution is remarkably consistent across Life, bioRxiv 2021.12.03.470944; doi: https://doi.org/10.1101/2021.12.03.470944

[18] Milo, R.; Phillips, R., Cell Biology by the Numbers, Garand Science (Taylor & Francis Group), pp 78-83, 2015.

[19] Abraham, F.F.; Singh, Y. The structure of a hard-sphere fluid in contact with a soft repulsive wall. J.Chem.Phys. 1977 **67**

[20] Kremer, K.; Grest, G.S., Dynamics of entangled linear melts: A molecular-dynamics simulation. J Chem Phys, 1990 **92** 5057.

[21] Aït Nouh M. et al., Twisted unknots Noeuds twistes. Acad. Sci. Paris, 2003 Ser. **I** 337.

[22] Amici, G.; Michele Caraglio, M.; Orlandini, E.; and Micheletti, C. Topological friction and relaxation dynamics of spatially confined catenated polymers. ACS Macro Lett. 2022, **11**, 1, 1–6